The Calcium-Sensor Guanylate Cyclase Activating Protein Type 2 Specific Site in Rod Outer Segment Membrane Guanylate Cyclase Type 1†

Teresa Duda,‡ Ewa Fik-Rymarkiewicz,‡,§ Venkateswar Venkataraman,‡,§ Ramalingam Krishnan,‡ Karl-Wilhelm Koch,|| and Rameshwar K. Sharma*,‡

Unit of Regulatory and Molecular Biology, Departments of Cell Biology and Ophthalmology, SOM and NJMS, University of Medicine and Dentistry of New Jersey, Stratford, New Jersey 08084, and AG Biochemistry, IBU, Faculty V, Carl von Ossietzky University, D-26111 Oldenburg, Germany

Received January 12, 2005; Revised Manuscript Received March 28, 2005

ABSTRACT: The rod outer segment membrane guanylate cyclase type 1 (ROS-GC1), originally identified in the photoreceptor outer segments, is a member of the subfamily of Ca^{2+}-modulated membrane guanylate cyclases. In phototransduction, its activity is tightly regulated by its two Ca^{2+}-sensor protein parts, GCAP1 and GCAP2. This study maps the GCAP2-modulatory site in ROS-GC1 through the use of multiple techniques involving surface plasmon resonance binding studies with soluble ROS-GC1 constructs, coimmunoprecipitation, functional reconstitution experiments with deletion mutants, and peptide competition assays. The findings show that the sequence motif of the core GCAP2-modulatory site is Y965−N981 of ROS-GC1. The site is distinct from the GCAP1-modulatory site. It, however, partially overlaps with the S100B-regulatory site. This indicates that the Y965−N981 motif tightly controls the Ca^{2+}-dependent specificity of ROS-GC1. Identification of the site demonstrates an intriguing topographical feature of ROS-GC1. This is that the GCAP2 module transmits the Ca^{2+} signals to the catalytic domain from its C-terminal side and the GCAP1 module from the distant N-terminal side.

Mammalian membrane-bound guanylate cyclases are composed of an extracellular and an intracellular domain linked by a single transmembrane region. They are divided into two subfamilies. Members of the first subfamily are activated through the extracellular region via hormones such as natriuretic peptides or bacterial toxins; those of the second, ROS-GC, are regulated by small Ca^{2+}-binding proteins that detect changes in cytoplasmic Ca^{2+} and act through the cytoplasmic part (reviewed in refs *1* and *2*). In addition, one form of the enzyme that shares sequence homology to hormone receptor guanylate cyclases is expressed in different rat and mouse tissues, but so far no activating ligand has been identified for this cyclase (*3*, *4*). The ROS-GC cyclases that are regulated by Ca^{2+} via Ca^{2+}-binding proteins are mainly, if not exclusively, expressed in neurosensory tissues or neurosensory-linked secondary neurons. Photoreceptor cells, for example, contain two guanylate cyclases, ROS-GC1 and ROS-GC2 (also termed GC-E and GC-F or retGC1 and retGC2, respectively), that are activated by guanylate cyclase activating proteins (GCAPs) when the cytoplasmic Ca^{2+} concentration decreases during a light response (reviewed in ref *2*). Thereby, they serve a key function in rod and cone physiology as they enhance synthesis of the second messenger cyclic GMP in a negative Ca^{2+}-feedback loop (reviewed in refs *1* and *5*).

Although up to eight different GCAP homologues have been described (most of them were found in teleost fish), the focus has been on GCAP1 and GCAP2 that are expressed in the mammalian retina (*6*−*11*). Both GCAPs are present in equimolar amounts in bovine rod outer segments (ROS) and regulate ROS-GC1 activity with almost equal affinity (*12*). However, GCAP1 and GCAP2 display different Ca^{2+} sensitivities (*12*), and only GCAP2 forms a dimer to activate ROS-GC1 (*13*). Furthermore, the covalently attached myristoyl group has a strong impact on regulatory properties of GCAP1 but has almost no effect on GCAP2 (*12*, *14*, *15*). These different regulatory modes that are mediated by GCAP1 and GCAP2 implicate two different target sites on ROS-GC1. In fact, initial mapping of regulatory sites for GCAP1 and GCAP2 has located the GCAP1 site to the N-terminal part and the GCAP2 site to the C-terminal part of the ROS-GC1 cytoplasmic domain (*16*, *17*). However, approaches to identify the interaction site of GCAP1 with ROS-GC1 resulted in the mapping of three different sites that were located on the juxtamembrane region (*18*), on the kinase homology region (*19*), and on the catalytic domain (*20*). So far, a similar effort to locate the binding site for GCAP2 has not been undertaken, although Sokal et al. (*20*) reported that the hypothetical GCAP1 binding site in the catalytic domain binds GCAP2 with a higher affinity than GCAP1. Furthermore, one study reports that GCAP2 interacts with the KHD of ROS-GC1 (*21*).

In the present study, a combination of different experimental strategies has been adopted to define the binding site

† This research was supported by USPHS Awards DC 005349 (R.K.S.) and HL 070015 (T.D.), a grant from the UMDNJ Foundation (V.V.), and a grant from the Deutsche Forschungsgemeinschaft (K.-W.K.).

* To whom correspondence should be addressed. Phone: 856-566-6977. Fax: 856-566-7057. E-mail: sharmark@umdnj.edu.

‡ University of Medicine and Dentistry of New Jersey.

§ These authors contributed equally to the work.

|| Carl von Ossietzky University.

10.1021/bi050068x CCC: $30.25
Published on Web 04/19/2005

for GCAP2 in ROS-GC1. Soluble ROS-GC1 constructs were expressed and used in binding assays such as surface plasmon resonance and coimmunoprecipitation. In vitro reconstitution experiments with deletion derivatives of ROS-GC1 were used in conjunction with peptide competition experiments to precisely define the structural and functional components of the GCAP2 binding site.

EXPERIMENTAL PROCEDURES

Antibodies. The detailed experiments demonstrating the specificities of antibodies against ROS-GC1, GCAP2, and GCAP1 have been published earlier (*22*−*25*).

Oligopeptides. Peptides covering the ROS-GC1 region V952−Q1022 were synthesized and purified according to ref *26*. These peptides were 20 aa long and overlapped by 10 aa with the preceding one.

ROS-GC1 Fragments. Expression and purification of the ROS-GC1 fragments aa M733−K1054 and aa Y965−K1054 were as described in refs *27* and *28*.

Surface Plasmon Resonance (SPR) Spectroscopy. Real-time binding analyses were performed at room temperature using the BIAcore X system. Two ROS-GC1 fragments, aa M733−K1054 and Y965−K1054, were tested. Each fragment was dissolved in 0.05 M sodium acetate buffer, pH 4.0, and coupled to the surface of a CM5 sensor chip via the primary amino group using the manufacturer's amine coupling protocol. The amount of immobilized protein was ~0.2 ng/mm^2. The running buffer for binding experiments contained 10 mM Tris-HCl, pH 7.5, 150 mM NaCl, 20 mM $MgCl_2$, 0.005% Surfactant P20, and, as appropriate, 1 mM EGTA or 1 mM $CaCl_2$ (final concentration). $MgCl_2$ (20 mM) in the running buffer was used in order to avoid binding of Ca^{2+} to the free carboxy groups within the dextran layer on the CM5 sensor chip (*29*). The flow rate was set to 15 μL/min. The control consisted of an independent flow cell on the same sensor that was subjected to a "blank immobilization" (no ROS-GC1 fragment was added in the process of chip preparation). The purified recombinant myristoylated GCAP2 was dissolved in the running buffer at varying concentrations (1.25−20 μM) and flushed over the experimental (ROS-GC1 fragment-coated) and control (uncoated) flow cells. Binding was observed as an increase in resonance units (RU). Maximal amplitudes were corrected by subtraction of the nonspecific binding (control flow cell). Regeneration was performed by short pulses (1 min) of 10 mM glycine, pH 2.5. The binding parameters, k_{on}, k_{off}, K_A, and K_D, for the interaction of GCAP2 with immobilized ROS-GC1 fragment were calculated using BIAevaluation 3.2 software. The curves were fitted according to a simple 1:1 interaction. A parameter for mass transfer was included to improve fitting in the case of fragment M733−K1054. The fitting residuals were minimal (−0.5 to 0.5) and showed very small systematic deviations.

ROS-GC1 Deletion Mutants. The ROS-GC1 deletion mutants, ΔP1016−K1054, ΔS972−K1054, ΔY965−K1054, and ΔR966−S972 (Figure 1), were constructed as described previously (*24*).

Expression Studies. COS-7 cells (simian virus 40-transformed African green monkey kidney cells), maintained in Dulbecco's modified Eagle's medium with penicillin, streptomycin, and 10% fetal bovine serum, were transfected

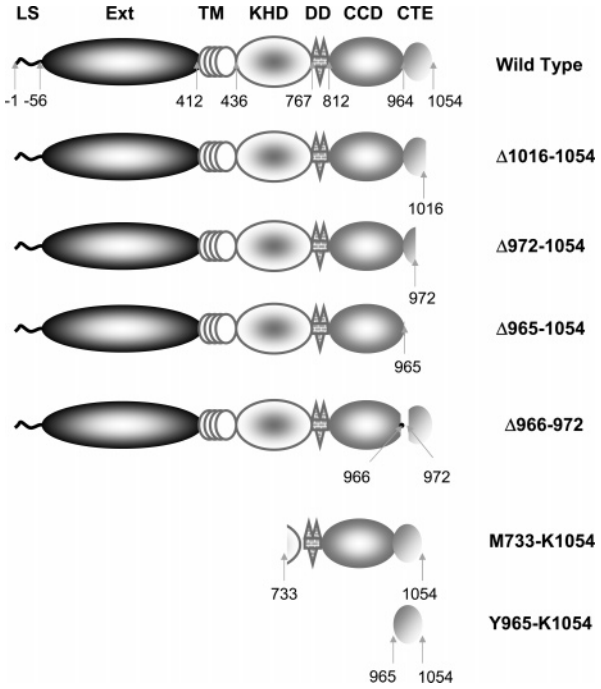

FIGURE 1: Schematic representation of ROS-GC1 and its deletion mutants. The following abbreviations denote the predicted domains: LS, leader sequence; Ext, extracellular domain; TM, transmembrane domain; DD, putative dimerization domain; CCD, cyclase catalytic domain; CTE, C-terminal extension. Numbers indicated correspond to the mature protein. The basal guanylate cyclase activities [pmol of cGMP min^{-1} (mg of protein)$^{-1}$] of ROS-GC1 and of the deletion mutants are almost identical (*24*).

with the wild-type recombinant or mutant ROS-GC1 expression constructs by the calcium phosphate coprecipitation technique (*30*). Sixty hours after transfection, cells were washed twice with 50 mM Tris-HCl (pH 7.5)/10 mM buffer, scraped into 2 mL of cold buffer, homogenized, centrifuged for 15 min at 5000*g*, and washed several times with the same buffer. The resulting pellet represented crude membranes.

Guanylate Cyclase Activity Assay. Membrane fractions were assayed for guanylate cyclase activity as described previously (*31*). Briefly, membranes were preincubated on an ice bath with or without GCAP2 in the assay system containing 10 mM theophylline, 15 mM phosphocreatine, 20 μg of creatine kinase, 50 mM Tris-HCl (pH 7.5), and 10 nM Ca^{2+}. The total assay volume was 25 μL. The reaction was initiated by the addition of the substrate solution containing 4 mM $MgCl_2$ and 1 mM GTP and maintained by incubation at 37 °C for 10 min. The reaction was terminated by the addition of 225 μL of 50 mM sodium acetate buffer (pH 6.2), followed by heating in a boiling water bath for 3 min. The amount of cyclic GMP formed was determined by radioimmunoassay (*32*).

Peptide Competition Experiments. Membranes of COS cells expressing ROS-GC1 were incubated with 10 μM GCAP2 and increasing concentrations of the peptides. Guanylate cyclase activity was assayed in the presence of 10 nM Ca^{2+} as described above.

Coimmunoprecipitation. Bacterially expressed and purified, soluble ROS-GC1 fragments, aa M733−K1054 or aaY965−K1054, and recombinant GCAPs were used. The fragment (2 μg) was incubated with 2 μg of GCAP1 or GCAP2 in the reaction buffer (20 mM Tris-HCl, pH 7.5, 150 mM NaCl, 1 mM PMSF, and 2 mM each of EDTA and

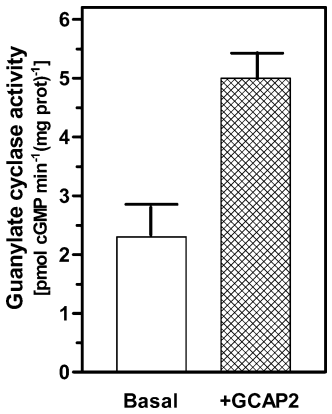

FIGURE 2: Functional integrity of the ROS-GC1 region aa M733−K1054. A protein corresponding to the ROS-GC1 region aa 733−1054 was expressed and purified as described in Experimental Procedures. This protein was tested for basal and GCAP2-dependent cyclase activity in the presence of 10 nM Ca^{2+}. The experiment was repeated two times with separate preparations of the protein.

EGTA) for 4 h at 4 °C. To minimize nonspecific interaction, 0.5% Triton X-100 was added to the reaction mixture (*33*). Immunoprecipitation was carried out for 6 h at 4 °C with affinity-purified ROS-GC1 antibody coupled to an agarose-bead matrix (2 μg of anti ROS-GC1 IgG/10 μL of Amino-Link plus coupling gel) according to the manufacturer's protocol (Pierce). The immunoprecipitated complexes were spun down and washed several times. Bound antigens were eluted using SDS sample buffer, separated on SDS−15% PAGE, and transferred onto nitrocellulose membranes. Triplicate samples were probed independently with specific antibodies against ROS-GC1, GCAP1, or GCAP2. The control experiment involved bacterially expressed and purified, soluble ONE-GC fragment M1022−C1110 (*37*), recombinant GCAP2, and anti-ONE-GC antibody (*37*). Immunoprecipitation was carried out as described above for ROS-GC1 fragments and GCAP2. Western blotting was carried out as described previously (*22*, *34*).

RESULTS

The C-Terminal Region of ROS-GC1, Amino Acids M733−K1054, Binds GCAP2. Systematic screening, through deletion mutations, has shown that the ROS-GC1 region amino acids (aa) Q731−K1054 is necessary and sufficient for the modulation by GCAP2 (*17*). To assess whether this segment binds GCAP2, its biological activity was ascertained first. The ROS-GC1 fragment aa M733−K1054 was expressed, purified to homogeneity, and analyzed for its biological activity: basal and GCAP2-modulated guanylate cyclase activity. The reason for the choice of the fragment M733−K1054 over Q731−K1054 was that the aa at position 733 is methionine and, thus, can serve as the translation start site for bacterial expression. The results presented in Figure 2 show that this ROS-GC1 fragment contains a basal guanylate cyclase activity of 2.3 pmol of cyclic GMP min^{-1} (mg of protein)$^{-1}$, which increases to 5 pmol of cyclic GMP min^{-1} (mg of protein)$^{-1}$ in the presence of 10 μM GCAP2 at 10 nM Ca^{2+}. Thus, the ROS-GC1 fragment aa M733−K1054 is biologically active and can be used for the direct binding studies.

Binding experiments were performed using SPR spectroscopy. Binding of GCAP2 to the immobilized ROS-GC1 fragment was observed as an increase in resonance units (RU). Since GCAP2 stimulates ROS-GC1 activity in the absence of Ca^{2+}, binding of GCAP2 to the ROS-GC1 fragment was determined initially in the presence of 1 mM EGTA. Incremental concentrations of GCAP2 (1.25−20 μM) resulted in a dose-dependent increase in binding of GCAP2 (Figure 3). A set of representative sensorgrams along with the respective curves derived after fitting to a 1:1 Langmuir binding model is presented in Figure 3A. The response at equilibrium (R_{eq}) was plotted as a function of GCAP2 concentration to determine the half-maximal binding (EC_{50}) of GCAP2 with ROS-GC1, which was 2.5 μM (Figure 3B). Analysis of the binding data (Scatchard transformation and BIAevaluation 3.2 software) yielded the K_D value of 2.2 μM. The EC_{50} and K_D values are in good agreement with the in vitro reconstitution experiments where 6−8 μM GCAP2 is required for half-maximal stimulation of ROS-GC1 expressed in COS cells (*17*). The other apparent binding parameters determined through the BIAevaluation software are as follows: k_{on} (association rate constant), 2.3×10^3 M^{-1} s^{-1}; k_{off} (dissociation rate constant), 5.1×10^{-3} s^{-1}; and K_A (equilibrium association constant), 4.5×10^5 M^{-1} (Table 1, fragment aa 733−1054 panel, $-Ca^{2+}$). These results indicate that the binding between GCAP2 and ROS-GC1 is of moderate affinity.

In the presence of micromolar concentrations of Ca^{2+}, GCAP2 inhibits ROS-GC1 activity (*12*, *36*). Therefore, it must also bind ROS-GC1 under these conditions. To determine whether the GCAP2 inhibitory binding site resides also within the ROS-GC1 region aa M733−K1054, the SPR binding experiments were performed in the presence of 1 mM Ca^{2+}. The results presented in Figure 3C show that the ROS-GC1 fragment binds GCAP2 under these conditions also. The observed half-maximal binding occurs at 2.5 μM GCAP2 (Figure 3C), and its calculated value is 2.6 μM. These affinity values as well as the other kinetic parameters for the interaction between ROS-GC1 fragment aa M733−K1054 and GCAP2 in the presence of Ca^{2+} are almost identical to those in its absence (Table 1, fragment aa 733−1054, $+Ca^{2+}$ vs $-Ca^{2+}$). These results demonstrate that GCAP2 binding to the ROS-GC1 fragment aa M733−K1054 is direct and is Ca^{2+}-independent. Thus, GCAP2 remains bound to ROS-GC1 irrespective of the presence of Ca^{2+}.

The SPR binding experiments were performed in the presence of 20 mM $MgCl_2$ in order to avoid binding of Ca^{2+} to the free carboxy groups within the dextran layer on the sensor chip resulting in changes in free Ca^{2+} concentration in the flow cell (*29*). However, since $MgCl_2$ has been recently shown to have an effect on GCAP-dependent regulation of ROS-GC activity (*35*), the binding (in the presence of 1 mM EGTA only) between GCAP2 and the aa M733−K1054 fragment of ROS-GC1 was measured without $MgCl_2$ in the running buffer. The half-maximal binding was at 2.8 μM GCAP2. Thus, $MgCl_2$ does not have any effect on GCAP2 binding to ROS-GC1 in the absence of Ca^{2+}.

Mapped GCAP2-Modulated Site in ROS-GC1. Based on reasoning that the ROS-GC1 region aa M733−P964 is highly (75−100%) conserved among all membrane guanylate cyclases and its respective segments, aa D767−A811 and E812−I864, contain common dimerization and catalytic domains, it was considered unlikely that this region contains the specialized GCAP2-modulated domain of ROS-GC1. For

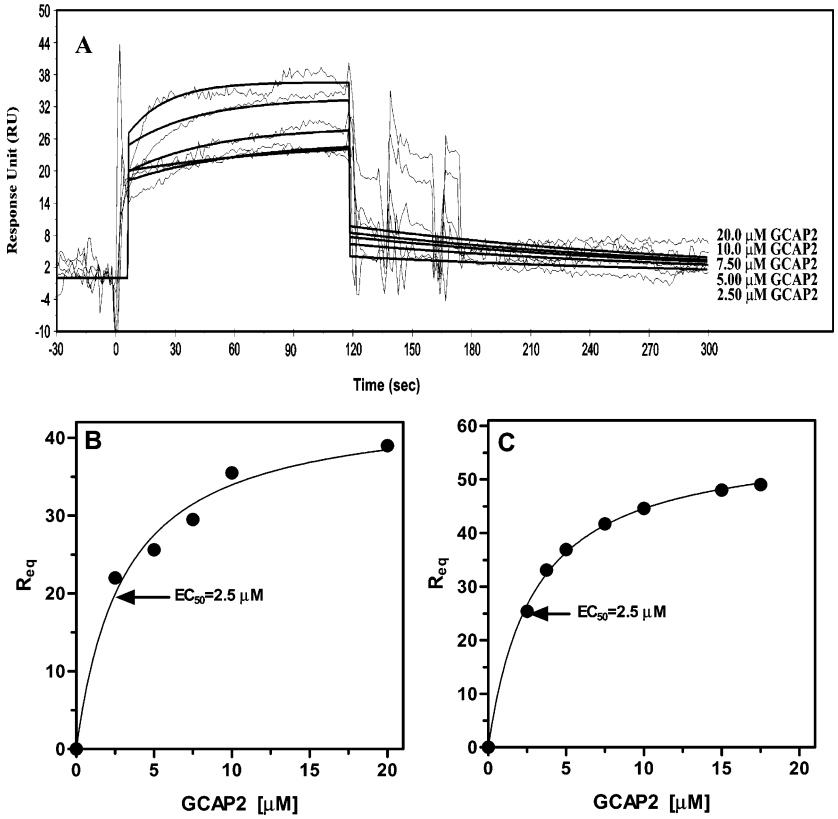

FIGURE 3: GCAP2 binding to ROS-GC1 fragment M733−K1054. Purified ROS-GC1 fragment aa M733−K1054 was immobilized on a CM5 sensor chip (BIAcore), and GCAP2 was supplied in the mobile phase at concentrations between 1.25 and 20 μM in running buffer. (A) Typical set of sensorgrams for GCAP2 binding in the presence of 1 mM EGTA overlaid with the respective curves after fitting to a 1:1 Langmuir model. The curves presented were obtained after the effect of buffers and salts on resonance signals was subtracted using the uncoated (blank) surface in flow cell 1 as a reference. (B) Binding data (R_{eq}) versus concentration of Ca^{2+}-free GCAP2 (1 mM EGTA was present in the running buffer). (C) Binding data (R_{eq}) versus concentration of Ca^{2+}-loaded GCAP2 (1 mM $CaCl_2$ was present in the running buffer). The experiment was repeated several times with different preparations of ROS-GC1 fragment immobilized on the chip and different preparations of GCAP2. The results presented are from one typical experiment.

Table 1: Kinetic Characteristics of ROS-GC1 Fragments' Interaction with GCAP2[a]

	fragment aa 733−1054		fragment aa 965−1054		peptide
	$-Ca^{2+}$	$+Ca^{2+}$	$-Ca^{2+}$	$+Ca^{2+}$	$-Ca^{2+}$
K_D (M)	2.2×10^{-6}	2.6×10^{-6}	2.1×10^{-6}	1.1×10^{-6}	1.9×10^{-6}
K_A (M^{-1})	4.5×10^{5}	3.7×10^{5}	4.7×10^{5}	8.9×10^{5}	5.2×10^{5}
k_{on} (M^{-1} s^{-1})	2.3×10^{3}	2.6×10^{3}	1.0×10^{3}	3.2×10^{3}	1.3×10^{3}
k_{off} (s^{-1})	5.1×10^{-3}	3.3×10^{-3}	2.0×10^{-3}	3.5×10^{-3}	2.5×10^{3}

[a] The ROS-GC1 fragments aa 733−1054 and 965−1054 or the peptide aa 963−985 was individually immobilized on a CM5 sensor chip, and GCAP2 (0−20 μM) was supplied in the mobile phase without or with 1 mM Ca^{2+} (for the peptide only without Ca^{2+}). The binding data were analyzed by BIAevaluation 3.2 software.

this reason, the aa fragment Y965−K1054 was analyzed for the presence of the GCAP2-modulated domain. The ROS-GC1 fragment was expressed, purified, and tested for GCAP2 binding through SPR. In these assays, the fragment immobilized on the sensor chip served as the stationary phase, and the increasing concentrations of GCAP2 (1−20 μM) in the absence of Ca^{2+} (1 mM EGTA) served as the mobile phase. A representative set of sensorgrams along with the respective curves derived after fitting to a 1:1 Langmuir binding model is presented (Figure 4A). Transformation of these data into equilibrium binding (R_{eq}) as a function of GCAP2 concentrations (Figure 4B) is also presented. Half-maximal binding was at 1.5 μM GCAP2, and the K_D value was calculated as 2.11 μM (Scatchard transformation and the BIAevaluation program). Other kinetic parameters were as follows: K_A, 4.7×10^5 M^{-1}; k_{on}, 1.0×10^3 M^{-1} s^{-1}; k_{off}, 2.0×10^{-3} s^{-1} (Table 1, fragment aa 965−1054 panel, $-Ca^{2+}$). Similar results were obtained when the binding experiments were performed in the presence of 1 mM Ca^{2+} (Figure 4C and Table 1, fragment aa 965−1054 panel, $+Ca^{2+}$). Thus, it is concluded that the ROS-GC1 region aa Y965−K1054 houses the GCAP2-binding domain.

To define the core GCAP2-binding domain, the first approach consisted of the functional analysis of the aa Y965−K1054 fragment of ROS-GC1. Starting from the C-terminus, three increasingly larger fragments, aa P1016−K1054, aa S972−K1054, and aa Y965−K1054, were removed from ROS-GC1. These mutants with the deleted portions (Figure 1) were expressed in COS cells and tested for their basal and GCAP2-dependent guanylate cyclase activities at 10 nM Ca^{2+} concentration. Identically treated membranes expressing wild-type ROS-GC1 were used as controls. The basal activities of all of these mutants are comparable, indicating that the deletions did not affect the integrity of the basal catalytic module of ROS-GC1 (*24*). As expected, the wild-type ROS-GC1 responded to GCAP2 in a dose-dependent fashion with an EC_{50} of 7 μM (Figure 5). The mutants, however, varied in their response patterns: ΔY965−K1054 was completely unresponsive; ΔS972−K1054 was about 50% responsive compared to the wild type,

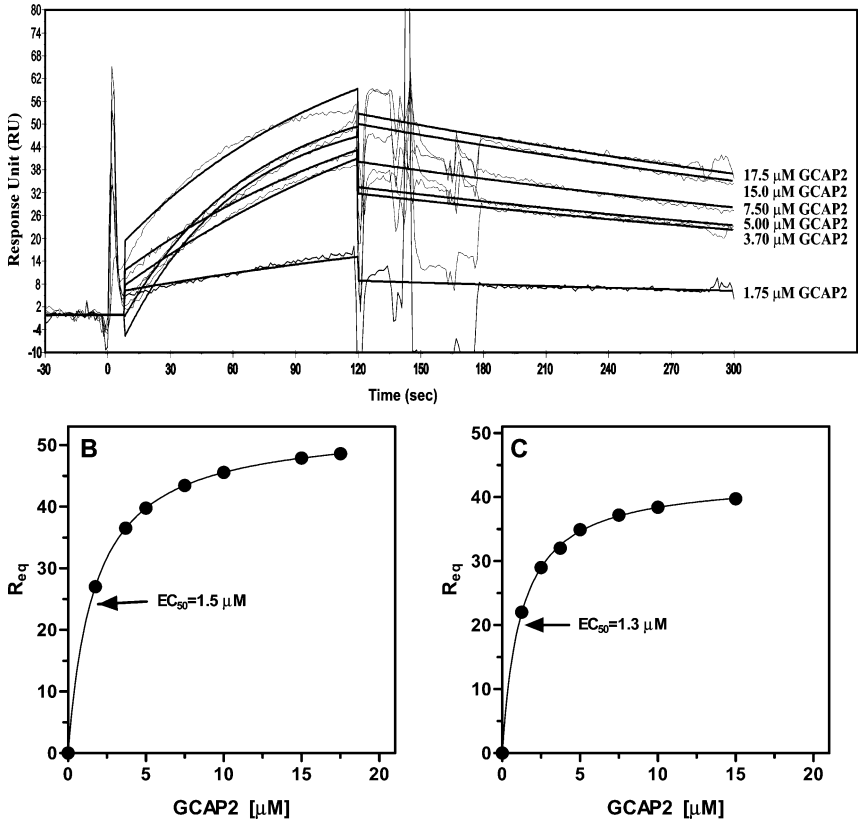

FIGURE 4: Binding of GCAP2 to ROS-GC1 fragment Y965−K1054. Purified ROS-GC1 fragment aa Y965−K1054 was immobilized on a CM5 sensor chip (BIAcore), and GCAP2 was supplied in the mobile phase. (A) Typical set of sensorgrams for GCAP2 binding in the presence of 1 mM EGTA overlaid with the respective curves after fitting to a 1:1 Langmuir model. The curves presented were obtained after the effect of buffers and salts on resonance signals was subtracted using the uncoated (blank) surface in flow cell 1 as a reference surface. (B) Binding data (R_{eq}) versus concentration of Ca^{2+}-free GCAP2 (1 mM EGTA was added to the running buffer). (C) Binding data (R_{eq}) versus concentration of Ca^{2+}-loaded GCAP2 (1 mM $CaCl_2$ was added to the running buffer). The experiment was repeated two times with different preparations of ROS-GC1 fragment immobilized on the chip and different preparations of GCAP2. The results presented are from one typical experiment.

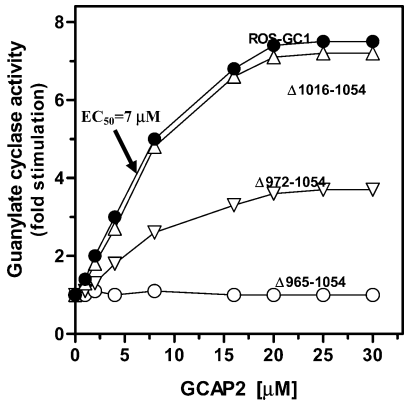

FIGURE 5: Mapping of the GCAP2-modulated region: effect of GCAP2 on the cyclase activity of ROS-GC1 and its deletion mutants. COS cells were individually transfected with ROS-GC1 or its deletion mutant (Δ1016−1054, Δ972−1054, and Δ965−1054) cDNA, and the cell particulate fractions were prepared as described in Experimental Procedures. These were assayed for guanylate cyclase activity in the presence of incremental concentrations of GCAP2 and 10 nM Ca^{2+}. The experiment was carried out in triplicate and repeated two times for reproducibility. The results presented are from one typical experiment. Error bars are within the size of the symbols.

and ΔP1016−K1054 responded identically to the wild-type ROS-GC1 (Figure 5). These results demonstrated that the functional GCAP2-modulated domain resides in the 52 aa, Y965−P1016, segment of ROS-GC1.

Peptide Competition Experiments. To further narrow down the GCAP2-modulated domain, the ROS-GC1 segment aa Y965−P1016 was subjected to peptide competition analyses. Overlapping, 20 aa long peptides covering the aa V952−L1021 region were screened for their competitive effects on GCAP2-dependent ROS-GC1 activity. For this purpose, membranes expressing wild-type ROS-GC1 were individually incubated with increasing concentrations of the peptides in the presence of GCAP2 and 10 nM Ca^{2+}, and cyclase activity was determined (Figure 6). Peptides V952−R971, G962−N981, and S972−R991 inhibited GCAP2-stimulated activity with differing efficiencies; peptides E982−E1001, T992−F1011, and T1002−Q1022, however, had no effect (Figure 6). The inhibition by peptide V952−R971 was ~60% with an IC_{50} of 100 μM, that by the peptide G962−N981 was ~90% with an IC_{50} of 70 μM, and that by the peptide S972−R991 was about 30% with an IC_{50} of 130 μM. These results indicated that the core GCAP2-modulated domain resides in the aa G962−N981 region of ROS-GC1. Together with the results of the SPR binding experiments, which demonstrate that the GCAP2-binding domain is in the aa Y965−K1054 fragment of ROS-GC1, it can now be inferred that the GCAP2-binding region is in the aa Y965−N981 segment of ROS-GC1.

This conclusion was validated by the direct binding experiments through SPR. The ROS-GC1 peptide corresponding to the aa L963−L985 segment was synthesized

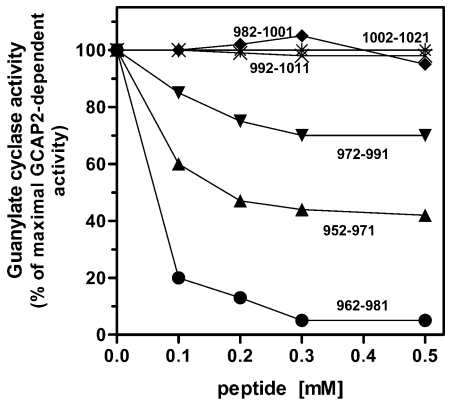

FIGURE 6: Inhibition of GCAP2-dependent ROS-GC1 activity as a function of peptide concentrations. Overlapping peptides covering the ROS-GC1 region aa V952−L1021 were synthesized as described in Experimental Procedures. Membranes of COS cells expressing ROS-GC1 were individually incubated with the incremental concentrations of the indicated peptides and 10 μM GCAP2 in the presence of 10 nM Ca^{2+}. Experiments were done in triplicate and repeated twice. The data shown are from one typical experiment. Error bars are within the size of the symbols.

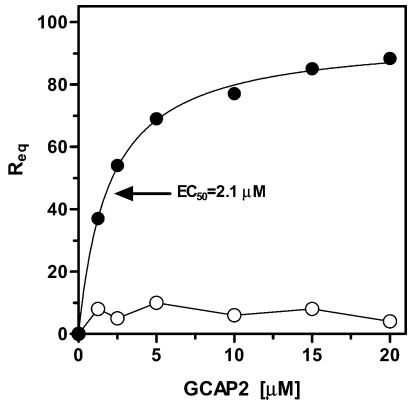

FIGURE 7: SPR analysis of GCAP2 binding to peptide aa L963−K985. A peptide corresponding to ROS-GC1 sequence aa L963−K985 was immobilized on a sensor chip, and GCAP2 was supplied in the running buffer (10 mM Tris-HCl, pH 7.5, 20 mM $MgCl_2$, 150 mM NaCl, 1 mM EGTA, 0.005% surfactant). Binding data (R_{eq}) versus the indicated concentrations of GCAP2 are presented (solid circles). A control experiment was performed under identical conditions with a corresponding peptide but with a scrambled sequence (open circles).

and assessed for GCAP2 binding. In comparison with the identified region Y965−N981, the peptide had additional residues both at N- and at C-terminal sites to allow better folding after attachment to the sensor chip. The control experiment involved the same peptide but with a scrambled sequence. The peptides were individually immobilized on a sensor chip, and incremental concentrations of GCAP2 were supplied in the mobile phase in the absence of free Ca^{2+} (presence of 1 mM EGTA). A transformation of the binding data (R_{eq}) versus GCAP2 concentrations is presented in Figure 7. For the peptide L963−L985, the half-maximal binding was at 2.1 μM GCAP2 (Figure 7, solid circles), and the calculated K_D is 1.9 μM. These values are comparable with those obtained for both of the previously described ROS-GC1 fragments (Table 1). The scrambled peptide did not exhibit any significant binding (Figure 7, open circles). Thus, these results show that the aa Y965−N981 region of ROS-GC1 contains the GCAP2-binding domain. Furthermore, it can now be concluded that this region defines both the structural and functional components of the GCAP2-modulated domain in ROS-GC1.

The GCAP2 Binding Site Is Distinct from the GCAP1 Binding Site in ROS-GC1. The original studies showed that the target sites of GCAP1 and GCAP2 in ROS-GC1 were on distinct regions of the cytoplasmic part of ROS-GC1 (*16*, *17*). These studies involved in vitro reconstitution experiments utilizing deletion and hybrid derivatives of ROS-GC1 expressed in COS cells and showed that (1) the GCAP1-modulated region resides in the region between aa R437 and I730 and (2) it is distinct from the GCAP2-modulated region, which resides between aa Q731 and K1054. By using a synthetic peptide library spanning the aa R437−G552 domain and site-directed mutagenesis, Lange et al. (*18*) identified two critical target regions in the juxtamembrane domain, M445−L456 and L503−I522, of ROS-GC1. The study concluded that the L503−I522 region represented the core GCAP1-binding domain. However, subsequent studies using different strategies showed three additional GCAP1 binding sites in ROS-GC1: S680−E699 and Q724−A738 (*19*) and G966−G983 (*20*).

With the information from the present study that the GCAP2 target site resides beyond aa M733 of ROS-GC1, the issue was raised: Does the aa M733−K1054 segment of ROS-GC1 contain the GCAP1 binding site? This issue was resolved by the coimmunoprecipitation experiments. GCAP1 or GCAP2 was incubated with the ROS-GC1 fragment aa M733−K1054 and the affinity-purified ROS-GC1 antibody coupled to gel as described (Experimental Procedures). The immunoprecipitated complexes were eluted and analyzed by Western blotting using antibodies against ROS-GC1, GCAP1, and GCAP2 (Figure 8). If the GCAP binds to the ROS-GC1 segment aa M733−K1054, it should be detected in the respective eluate. The eluate contained the ROS-GC1 fragment aa M733−K1054 of molecular mass ~40 kDa (Figure 8, lanes 1and 2; indicated by an arrowhead). It contained GCAP2 (Figure 8, lane 4; indicated by an arrowhead). However, no GCAP1 was detected (Figure 8A, lane 6). These results clearly show that GCAP2 binds to the ROS-GC1 fragment aa M733−K1054, while GCAP1 does not. As expected, identical results were obtained when the ROS-GC1 fragment aa Y965−K1054 was used (not shown). To verify that GCAP2 binding to the ROS-GC1 fragment aa Y965−K1054 is specific, a coimmunoprecipitation experiment was performed using the corresponding region (M1022−C1110) of another Ca^{2+}-modulated membrane guanylate cyclase, ONE-GC (*37*). Until now, the only known modulator of ONE-GC activity is neurocalcin δ (*37*). The immunoprecipitated complexes were analyzed by Western blotting using antibodies against ONE-GC and GCAP2. GCAP2 was not detected in these complexes (Figure 8B). Thus, the results from the coimmunoprecipitation experiments demonstrate that (1) GCAP2 interaction with the ROS-GC1 fragment aa Y965−K1054 is specific and (2) the ROS-GC1 region M733−K1054 contains the binding site for GCAP2 but not for GCAP1.

The conclusions of the immunoprecipitation experiment were further validated by the functional studies involving deletion mutants. Deletion mutants of ROS-GC1 spanning the region Y965−K1054 were tested for their responsiveness to GCAP1. The response of all the mutants was identical to that of the wild-type ROS-GC1 (Figure 8C). These results

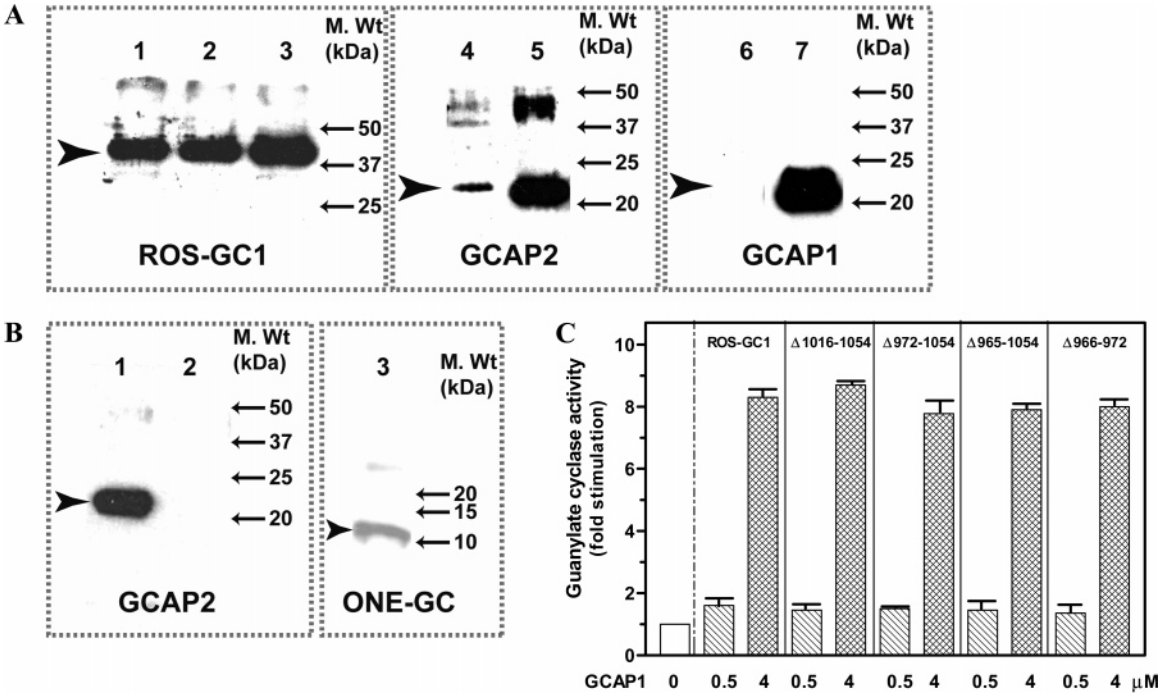

FIGURE 8: ROS-GC1 fragment aa M733−K1054 binds GCAP2 but not GCAP1. (A) Coimmunoprecipitation. The ROS-GC1 region aa M733−K1054, GCAP2, and GCAP1 were expressed and purified as described in Experimental Procedures. 2 μg of the ROS-GC1 fragment was incubated with 2 μg of GCAP2 or GCAP1 for 4 h at 4 °C in a buffer consisting of 20 mM Tris-HCl, pH 7.5, 150 mM NaCl, 0.5% Triton X-100, and 1 mM PMSF in the presence of 2 mM EGTA/2 mM EDTA. After addition of anti-ROS-GC1 antibody coupled to AminoLink plus coupling gel (Pierce) to the reaction mixture, the incubation was continued for 6 h. The immunoprecipitated complexes were separated from the beads, electrophoresed on SDS−polyacrylamide gels, and analyzed by Western blotting with anti-ROS-GC1 antibody (panel ROS-GC1, lane 1), anti-GCAP2 antibody (panel GCAP2, lane 4), and anti-GCAP1 antibody (panel GCAP1, lane 6). The ROS-GC1 fragment incubated without GCAP1 or GCAP2 with anti-ROS-GC1 antibody coupled to AminoLink plus coupling gel and then separated (lane 2), ROS-GC1 fragment alone (lane 3), recombinant GCAP2 alone (lane 5), and GCAP1 alone (lane 7) were electrophoresed and analyzed in parallel as controls. The immunoreactive bands are indicated in each panel. (B) Specificity of GCAP2 binding. ONE-GC fragment aa M1022−C1110 was expressed, purified to homogeneity (*37*), and used with GCAP2 for coimmunoprecipitation experiments. The experiment was done as described in (A) except that anti ONE-GC antibody was used. The specificity of anti ONE-GC antibody is described in ref *37*. Lanes: 1, recombinant GCAP2 alone; 2, immunoprecipitated GCAP2; 3, ONE-GC fragment. The immunoreactive bands are indicated in each panel. (C) GCAP1-dependent activation of ROS-GC1 and its deletion mutants. COS cells were individually transfected with ROS-GC1 or its deletion mutant (Δ1016−1054, Δ972−1054, and Δ965−1054) cDNA, and the cell particulate fractions were prepared as described in Experimental Procedures. These were assayed for guanylate cyclase activity in the presence of 0.5 or 4 μM GCAP1 and 10 nM Ca^{2+}. The experiment was carried out in triplicate and repeated two times for reproducibility.

show that the GCAP1-modulatory domain does not reside within the ROS-GC1 C-terminal region aa Y965−K1054 (Figure 8C and Figure 9 in ref *24*). Thus, the GCAP2 binding site is distinct from the GCAP1 binding site in ROS-GC1.

The GCAP2 Binding Site Overlaps with, yet Is Not Identical to, the S100B Binding Site. S100B is another Ca^{2+}-sensor component of ROS-GC1. However, in contrast to GCAPs, it stimulates ROS-GC1 with an EC_{50} value of 0.75 μM for Ca^{2+}. The core S100B binding site resides in the aa segment R966−S972 of ROS-GC1 (*24*). With the present finding that the aa Y965−N981 constitutes the GCAP2 binding site, it became clear that the core GCAP2- and S100B-binding domains in ROS-GC1 might overlap. To assess the extent of the overlap, two strategies, deletion mutation and competitive inhibition, were used. The conclusions arrived at through both strategies were identical. In the deletion mutation strategy, the core S100B-binding domain, aa R966−S972, was deleted from ROS-GC1, the mutant was expressed in COS cells, and its GCAP2 responsiveness was assessed. Compared to the wild-type ROS-GC1, the mutant's response to GCAP2 was ~60% lower (Figure 9A). There are two possible interpretations of these results: (1) the region R966−S972 is important for the binding of GCAP2 or (2) this region does not bind GCAP2, but its deletion causes a conformational change that decreases the ROS-GC1 response to GCAP2. The second interpretation, however, is not valid because (1) the mutant is fully responsive to GCAP1 (Figure 8C), indicating that the lowered response to GCAP2 is an intrinsic property of the protein and not the effect of a defective folding caused by the deletion, and (2) the results from the direct binding and peptide competition experiments demonstrate that the L963−L985 region binds GCAP2 (Table 1 and Figure 7). Thus, the R966−S972 region is important for GCAP2 binding. Since the R966−S972 region is also involved in S100B binding (*24*), these results indicate that the core GCAP2 and S100B binding sites partially overlap.

In the competitive inhibition strategy, membranes of COS cells expressing wild-type ROS-GC1 were preincubated with saturated amounts of GCAP2 (10 μM) in the presence of saturated amounts of Ca^{2+} (100 μM). They were then tested for their dose-dependent response to S100B (Figure 9B). The control membranes passed through the same operational steps but without the GCAP2 preincubation step. The treated membranes showed ~40% less stimulation of guanylate cyclase activity compared to the control. In addition, the EC_{50} value for GCAP2 shifted from 0.8 to 1.2 μM upon treatment. These results are consistent with the above results from the

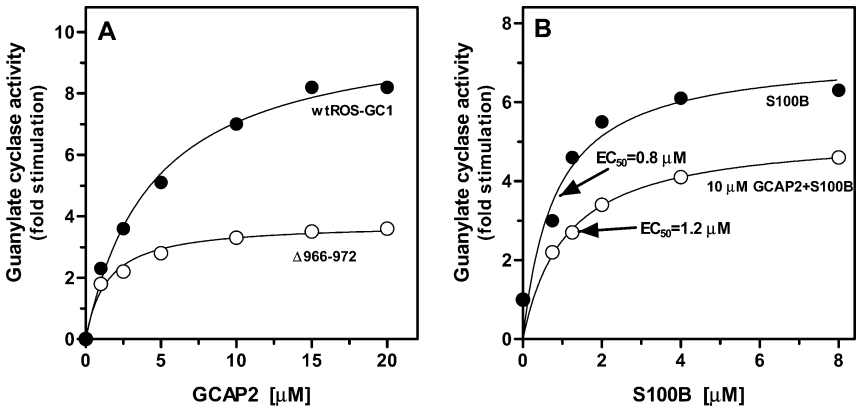

FIGURE 9: GCAP2 binding site in ROS-GC1 partially overlaps with S100B recognition site. (A) Membranes of COS cells expressing ROS-GC1 or its mutant Δ966−972 (deleted the S100B recognition sequence; refs *24* and *38*) were assayed for guanylate cyclase activity in the presence of incremental concentrations of GCAP2 and 10 nM Ca^{2+}. The experiment was carried out in triplicate and repeated two times for reproducibility. The results presented are from one typical experiment. Error bars are within the size of the symbols. (B) Membranes of COS cells expressing ROS-GC1 were preincubated for 10 min on an ice bath with (open circles) or without (closed circles) 10 μM GCAP2 in the presence of 100 μM $CaCl_2$. Incremental concentrations of S100B were added to the reaction mixture, and the guanylate cyclase activity was assayed. The experiment was repeated two times for reproducibility. Error bars are within the size of the symbols.

deletion mutation studies and previous results on the S100B-modulatory site in ROS-GC1 (*24*) and indicate that the ROS-GC1 region aa Y965−N981 contains both GCAP2 and S100B binding sites. An alternative possibility, if these experiments were considered in isolation, is that GCAP2 and S100B bind at different sites and the observed effect is due to stimulation of ROS-GC1 by S100B and inhibition by GCAP2. However, on the basis of results from competition and binding experiments with peptides, the alternative interpretation is considered a remote possibility.

DISCUSSION

Through the means of a comprehensive technology involving the use of soluble constructs of ROS-GC1, direct binding measurements by SPR, coimmunoprecipitation, and finally functional reconstitution experiments utilizing progressive deletion constructs and peptide competition, this study defines the Ca^{2+}-sensor GCAP2-modulated site in ROS-GC1. The site is absolutely specific for GCAP2 and does not overlap with the GCAP1-modulated site. This clarifies the existing confusion in the literature that the two GCAPs' sites overlap. The identity of the mapped GCAP2-modulated site defines a new topography of ROS-GC1. In this topography, the catalytic module of ROS-GC1 is flanked by the GCAP1-modulated domain at its N-terminal site and by the GCAP2-modulated domain at its C-terminal site. The identity of the site reveals its most curious structural feature. It overlaps with the S100B-modulated site of ROS-GC1. This indicates that only a small structural variation in the site converts ROS-GC1 from the Ca^{2+}-inhibitory mode to the Ca^{2+}-stimulatory mode. These findings are elaborated below.

The Modulation of ROS-GC1 by GCAP2 Is Specific and Occurs through a Defined Structural Motif. In the present study, systematic screening of the Q731−K1054 region of ROS-GC1 has revealed that the core binding domain of GCAP2 resides in the aa Y965−N981. The binding constants show that Ca^{2+} has no effect on the affinity of GCAP2 for ROS-GC1. GCAP2 binds ROS-GC1 with similar affinities in the presence and absence of Ca^{2+} with respective K_D values of 3.1×10^{-6} and 2.6×10^{-6} M. The kinetic parameters (Table 1) indicate that GCAP2 interaction, binding as well as dissociation, with ROS-GC1 is Ca^{2+}-independent, direct, and of moderate affinity.

Thus, the findings of the present study support a model in which light-dependent changes in free Ca^{2+} trigger a conformational change in GCAP2 and subsequently in ROS-GC1. This "activator-to-inhibitor transition" (*36*) operates without discrete association, dissociation, and diffusion steps; instead, it allows a fast response according to varying free Ca^{2+}. Thereby, operation of GCAP2 is reminiscent of GCAP1 targeting on ROS-GC1 (reviewed in ref *1*).

Given the similarity in regulatory modes of the two GCAPs, the following two questions arise: 1. Does the GCAP2-modulated domain overlap with the GCAP1-modulated domain? 2. Do the two domains reside at the C-terminal region of ROS-GC1? With respect to conflicting results in the literature, these issues have been revisited in the present investigation and have been resolved through the coimmunoprecipitation technique.

The affinity-purified ROS-GC1 antibody coprecipitated the ROS-GC1 fragment aa M733−K1054 and GCAP2. However, it did not coprecipitate GCAP1 with this fragment. Thus, the M733−K1054 region of ROS-GC1 contains the GCAP2 binding site and not the GCAP1 site. As anticipated, similar results were obtained with the Y965−K1054 fragment of ROS-GC1. These results are in agreement with a previous investigation showing that the GCAP1-regulatory site is located outside the Y965−K1054 region of ROS-GC1 (*24*). These results establish that the two sites do not overlap, they are separate, and the GCAP1 site does not reside at the C-terminus of ROS-GC1, which includes the Y965−N981 segment of ROS-GC1.

Identification of the GCAP2-Modulated Site at the C-Terminal Region Shows a New Topography of ROS-GC1 (Figure 10). The knowledge that the GCAP1- and GCAP2-modulated sites exist at the two opposite ends of the catalytic module of ROS-GC1 results in the revised topographic model of ROS-GC1. In this model, the two modules of ROS-GC1 are independently modulated by the Ca^{2+} impulses. The critical feature of the model is that the independence of the two modules is incurred by the orientation of the modules around the catalytic domain of ROS-GC1. The GCAP1

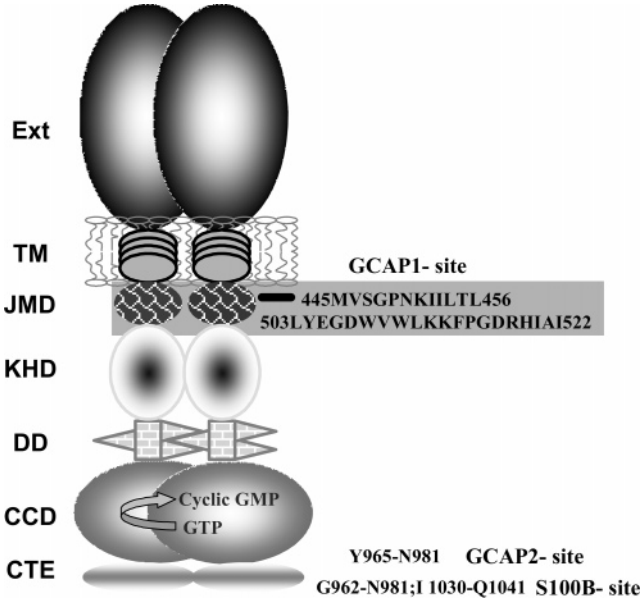

FIGURE 10: Topography of ROS-GC1. A schematic diagram of ROS-GC1, with its multiple domains shaded differently, is provided. The extracellular domain (Ext), the transmembrane (TM), the juxtamembrane (JMD), the kinase homology (KHD), the putative dimerization (DD), the catalytic core (CCD), and the C-terminal extension (CTE) domains have been identified. The GCAP1-, GCAP2-, and S100B-binding domains are indicated.

module transmits the Ca^{2+} signals to the catalytic domain from its C-terminal side and the GCAP1 module from the distant N-terminal side. In this manner both modules tightly control the light-dependent Ca^{2+} sensitivity of ROS-GC1.

Only a Small Structural Variation Exists between the GCAP2 and S100B Ca^{2+} Switches in ROS-GC1. An intriguing structural/functional feature of the GCAP2-modulated Ca^{2+} switch in ROS-GC1 is that it overlaps and is only minimally different from the S100B-modulated switch. This indicates that the individual amino acid residues present in the Y965−N981 motif of ROS-GC1 tightly control the Ca^{2+}-dependent specificity of ROS-GC1. The control is so delicate that only very few (or even single) amino acids convert the cyclase from being Ca^{2+}-inhibited, as in the case of GCAP2, to being Ca^{2+}-stimulated, as is the case with S100B. The future task therefore will be to analyze the role of the individual amino acids in the structural motif for control of the Ca^{2+}-dependent stimulation or inhibition of ROS-GC1.

In conclusion, the present study demonstrates, for the first time, direct binding of GCAP2 to ROS-GC1 and provides a detailed kinetic analysis of the ROS-GC1 and GCAP2 interaction. It further establishes that this interaction of moderate affinity is Ca^{2+}-independent. It precisely defines the ROS-GC1 region Y965−N981 that represents the binding site for GCAP2. In contrast to GCAP1 and S100B sites, which are composed of noncontiguous binding and transduction regions, the Y965−N981 region of ROS-GC1 houses both the structural and functional components that mediate GCAP2 regulation.

REFERENCES

1. Koch, K. W., Duda, T., and Sharma, R. K. (2002) Photoreceptor specific guanylate cyclases in vertebrate phototransduction, *Mol. Cell. Biochem. 230*, 97−106.
2. Sharma, R. K. (2002) Evolution of the membrane guanylate cyclase transduction system, *Mol. Cell. Biochem. 230*, 3−30.
3. Schulz, S., Wedel, B. J., Matthews, A., and Garbers, D. L. (1998) The cloning and expression of a new guanylyl cyclase orphan receptor, *J. Biol. Chem. 273*, 1032−1037.
4. Kuhn, M., Ng, C. K., Su, Y. H., Kilic, A., Mitko, D., Bien-Ly, N., Komuves, L. G., and Yang, R. B. (2004) Identification of an orphan guanylate cyclase receptor selectively expressed in mouse testis, *Biochem. J. 379*, 385−393.
5. Pugh, E. N., Jr., Duda, T., Sitaramayya, A., and Sharma, R. K. (1997) Photoreceptor guanylate cyclases: a review, *Biosci. Rep. 17*, 29−73.
6. Palczewski, K., Subbaraya, I., Gorczyca, W. A., Helekar, B. S., Ruiz, C. C., Ohguro, H., Huang, J., Zhao, X., Crabb, J. W., Johnson, R. S., and Baehr, W. (1994) Molecular cloning and characterization of retinal photoreceptor guanylyl cyclase-activating protein, *Neuron 13*, 395−404.
7. Dizhoor, A. M., Lowe, D. G., Olshevskaya, E. V., Laura, R. P., and Hurley, J. B. (1994) The human photoreceptor membrane guanylyl cyclase, RetGC, is present in outer segments and is regulated by calcium and a soluble activator, *Neuron 12*, 1345−1352.
8. Dizhoor, A. M., Olshevskaya, E. V., Henzel, W. J., Wong, S. C., Stults, J. T., Ankoudinova, I., and Hurley, J. B. (1995) Cloning, sequencing, and expression of a 24-kDa Ca^{2+}-binding protein activating photoreceptor guanylyl cyclase, *J. Biol. Chem. 270*, 25200−25206.
9. Frins, S., Bonigk, W., Muller, F., Kellner, R., and Koch, K.-W. (1996) Functional characterization of a guanylyl cyclase-activating protein from vertebrate rods. Cloning, heterologous expression, and localization, *J. Biol. Chem. 271*, 8022−8027.
10. Imanishi, Y., Sokal, I., Sowa, M. E., Lichtarge, O., Wensel, T. G., Saperstein, D. A., Baehr, W., and Palczewski, K. (2002) Characterization of retinal guanylate cyclase-activating protein 3 (GCAP3) from zebrafish to man, *Eur. J. Neurosci. 15*, 63−78.
11. Imanishi, Y., Yang, L., Sokal, I., Filipek, S., Palczewski, K., and Baehr, W. (2004) Diversity of guanylate cyclase-activating proteins (GCAPs) in teleost fish: characterization of three novel GCAPs (GCAP4, GCAP5, GCAP7) from zebrafish (Danio rerio) and prediction of eight GCAPs (GCAP1−8) in pufferfish (Fugu rubripes), *J. Mol. Evol. 59*, 204−217.
12. Hwang, J.-Y., Lange, C., Helten, A., Höppner-Heitmann, D., Duda, T., Sharma, R. K., and Koch, K.-W. (2003) Regulatory modes of rod outer segment membrane guanylate cyclase differ in catalytic efficiency and Ca^{2+}-sensitivity, *Eur. J. Biochem. 270*, 3814−3821.
13. Olshevskaya, E. V., Ermilov, A. N., and Dizhoor, A. M. (1999) Dimerization of guanylyl cyclase-activating protein and a mechanism of photoreceptor guanylyl cyclase activation, *J. Biol. Chem. 274*, 25583−25587.
14. Olshevskaya, E. V., Hughes, R. E., Hurley, J. B., and Dizhoor, A. M. (1997) Calcium binding, but not a calcium-myristoyl switch, controls the ability of guanylyl cyclase-activating protein GCAP-2 to regulate photoreceptor guanylyl cyclase, *J. Biol. Chem. 272*, 14327−14333.
15. Hwang, J. Y., and Koch, K.-W. (2002) Calcium- and myristoyl-dependent properties of guanylate cyclase-activating protein-1 and protein-2, *Biochemistry 41*, 13021−13028.
16. Duda, T., Goraczniak, R., Surgucheva, I., Rudnicka-Nawrot, M., Gorczyca, W. A., Palczewski, K., Sitaramayya, A., Baehr, W., and Sharma, R. K. (1996) Calcium modulation of bovine photoreceptor guanylate cyclase, *Biochemistry 35*, 8478−8482.
17. Krishnan, A., Goraczniak, R. M., Duda, T., and Sharma, R. K. (1998) Third calcium-modulated rod outer segment membrane guanylate cyclase transduction mechanism, *Mol. Cell. Biochem. 178*, 251−259.
18. Lange, C., Duda, T., Beyermann, M., Sharma, R. K., and Koch, K.-W. (1999) Regions in vertebrate photoreceptor guanylyl cyclase ROS-GC1 involved in Ca^{2+}-dependent regulation by guanylyl cyclase-activating protein GCAP-1, *FEBS Lett. 460*, 27−31.
19. Krylov, D. M., and Hurley, J. B. (2001) Identification of proximate regions in a complex of retinal guanylyl cyclase 1 and guanylyl cyclase-activating protein-1 by a novel mass spectrometry-based method, *J. Biol. Chem. 276*, 30648−30654.
20. Sokal, I., Haeseleer, F., Arendt, A., Adman, E. T., Hargrave, P. A., and Palczewski, K. (1999) Identification of a guanylyl cyclase-activating protein-binding site within the catalytic domain of retinal guanylyl cyclase 1, *Biochemistry 38*, 1387−1393.
21. Laura, R. P., and Hurley, J. B. (1998) The kinase homology domain of retinal guanylyl cyclases 1 and 2 specifies the affinity and cooperativity of interaction with guanylyl cyclase activating protein-2, *Biochemistry 37*, 11264−11271.

22. Venkataraman, V., Nagele, R., Duda, T., and Sharma, R. K. (2000) Rod outer segment membrane guanylate cyclase type 1-linked stimulatory and inhibitory calcium signaling systems in the pineal gland: Biochemical, molecular, and immunohistochemical evidence, *Biochemistry 39*, 6042−6052.
23. Venkataraman, V., Duda, T., Vardi, N., Koch, K.-W., and Sharma, R. K. (2003) Calcium-modulated guanylate cyclase transduction machinery in the photoreceptor−bipolar synaptic region, *Biochemistry 42*, 5640−5648.
24. Duda, T., Koch, K.-W., Venkataraman, V., Lange, C., Beyermann, M., and Sharma, R. K. (2002) Ca^{2+} sensor S100beta-modulated sites of membrane guanylate cyclase in the photoreceptor-bipolar synapse, *EMBO J. 21*, 2547−2556.
25. Goraczniak, R. M., Duda, T., and Sharma, R. K. (1998) Calcium modulated signaling site in type 2 rod outer segment membrane guanylate cyclase (ROS-GC2), *Biochem. Biophys. Res. Commun. 245*, 447−453.
26. Zoche, M., Bienert, M., Beyermann, M., and Koch, K.-W. (1996) Distinct molecular recognition of calmodulin-binding sites in the neuronal and macrophage nitric oxide synthases: a surface plasmon resonance study, *Biochemistry 35*, 8742−8747.
27. Duda, T., Venkataraman, V., Jankowska, A., Lange, C., Koch, K.-W., and Sharma, R. K. (2000) Impairment of the rod outer segment membrane guanylate cyclase dimerization in a cone-rod dystrophy results in defective calcium signaling, *Biochemistry 39*, 12522−12533.
28. Krishnan, A., Venkataraman, V., Fik-Rymarkiewicz, E., Duda, T., and Sharma, R. K. (2004) Structural, biochemical, and functional characterization of the calcium sensor neurocalcin delta in the inner retinal neurons and its linkage with the rod outer segment membrane guanylate cyclase transduction system, *Biochemistry 43*, 2708−2723.
29. Lange, C., and Koch, K.-W. (1997) Calcium-dependent binding of recoverin to membranes monitored by surface plasmon resonance spectroscopy in real time, *Biochemistry 36*, 12019−12026.
30. Sambrook, M. J., Fritsch, E. F., and Maniatis, T. (1989) *Molecular Cloning: A Laboratory Manual*, Cold Spring Harbor Laboratory, Cold Spring Harbor, NY.
31. Paul, A. K., Marala, R. B., Jaiswal, R. K., and Sharma, R. K. (1987) Coexistence of guanylate cyclase and atrial natriuretic factor receptor in a 180-kD protein, *Science 235*, 1224−1226.
32. Nambi, P., Aiyar, N. V., and Sharma, R. K. (1982) Adrenocorticotropin-dependent particulate guanylate cyclase in rat adrenal and adrenocortical carcinoma: comparison of its properties with soluble guanylate cyclase and its relationship with ACTH-induced steroidogenesis, *Arch. Biochem. Biophys. 217*, 638−646.
33. Ausubel, F. M., Brent, R., Kingston, R. E., Moore, D. D., Seidman, J. G., Smits J. A., and Struhl, K., Eds. (1996) *Current Protocols in Molecular Biology*, Chapter 10, John Wiley & Sons, New York.
34. Duda, T., Venkataraman, V., Krishnan, A., Nagele, R. G., and Sharma, R. K. (2001) Negatively calcium-modulated membrane guanylate cyclase signaling system in the rat olfactory bulb, *Biochemistry 40*, 4654−4662.
35. Peshenko, I. V., and Dizhoor, A. M. (2004) Guanylyl cyclase-activating proteins (GCAPs) are Ca^{2+}/Mg^{2+} sensors: implications for photoreceptor guanylyl cyclase (RetGC) regulation in mammalian photoreceptors, *J. Biol. Chem. 279*, 16903−16906.
36. Dizhoor, A. M., and Hurley, J. B. (1996) Inactivation of EF-hands makes GCAP-2 (p24) a constitutive activator of photoreceptor guanylyl cyclase by preventing a Ca^{2+}-induced "activator-to-inhibitor" transition, *J. Biol. Chem. 271*, 19346−19350.
37. Duda, T., Fik-Rymarkiewicz, E., Venkataraman, V., Krishnan, A., and Sharma, R. K. (2004) Calcium-modulated ciliary membrane guanylate cyclase transduction machinery: constitution and operational principles, *Mol. Cell. Biochem. 267*, 107−122.
38. Ivanenkov, V. V., Jamieson, G. A., Jr., Gruenstein, E., and Dimlich, R. V. (1995) Characterization of S-100b binding epitopes. Identification of a novel target, the actin capping protein, CapZ, *J. Biol. Chem. 270*, 14651−14658.

BI050068X